Transition from Contraction to Extension in the Northeastern Basin and Range: New Evidence from the Copper Mountains, Nevada

Author(s): Jeffrey M. Rahl, Allen J. McGrew and Kenneth A. Foland

Source: *The Journal of Geology*, Vol. 110, No. 2 (March 2002), pp. 179-194
Published by: The University of Chicago Press
Stable URL: http://www.jstor.org/stable/10.1086/338413
Accessed: 12-03-2017 17:41 UTC

Transition from Contraction to Extension in the Northeastern Basin and Range: New Evidence from the Copper Mountains, Nevada

Jeffrey M. Rahl,[1] *Allen J. McGrew,*[2] *and Kenneth A. Foland*[3]

Department of Geology, University of Dayton, Dayton, Ohio 45469-2364, U.S.A.

ABSTRACT

New mapping, structural analysis, and $^{40}Ar/^{39}Ar$ dating reveal an unusually well-constrained history of Late Eocene extension in the Copper Mountains of the northern Basin and Range province. In this area, the northeast-trending Copper Creek normal fault juxtaposes a distinctive sequence of metacarbonate and granitoid rocks against a footwall of Upper Precambrian to Lower Cambrian quartzite and phyllite. Correlation of the hanging wall with footwall rocks to the northwest provides an approximate piercing point that requires 8–12 km displacement in an ESE direction. This displaced fault slice is itself bounded above by another normal fault (the Meadow Fork Fault), which brings down a hanging wall of dacitic to rhyolitic tuff that grades conformably upward into conglomerate. These relationships record the formation of a fault-bounded basin between 41.3 and 37.4 Ma. The results are consistent with a regional pattern in which volcanism and extension swept southward from British Columbia to southern Nevada from Early Eocene to Late Oligocene time. Because the southward sweep of volcanism is thought to track the steepening and foundering of the downgoing oceanic plate, these results suggest that the crucial mechanisms for the onset of regional extension were probably changes in plate boundary conditions coupled with convective removal of mantle lithosphere and associated regional magmatism and lithospheric weakening. Paleobotanical data indicate that surface elevations in northeastern Nevada were not significantly different than at present, suggesting that gravitational instability of overthickened continental crust was not the dominant force driving the onset of crustal thinning in mid-Tertiary time.

Introduction

During Late Cretaceous time, the Cordilleran margin of North America experienced an episode of contractional tectonics, the Sevier orogeny (Armstrong 1968), that contrasts greatly with the widespread extension that ultimately formed the Basin and Range province in Cenozoic time. Considerable debate exists regarding the mechanisms responsible for this transition from regional contraction to extension (see review by Sonder and Jones 1999). Several workers argue that Paleogene extension resulted from a release of potential energy associated with Mesozoic crustal thickening (Coney and Harms 1984; Axen et al. 1993; Janecke 1994; Wells 1997; Jones et al. 1998). Others propose that widespread magmatism was critical, either in driving active rifting or in thermally weakening the lithosphere so that rifting could occur due to either back-arc extension or gravitational collapse (Gans et al. 1989; Armstrong and Ward 1991).

Regardless of other mechanisms, evolving Cordilleran plate boundary conditions undoubtedly played an important direct or indirect role in triggering Late Paleogene extension. For example, relative convergence rates at the plate margin began to decelerate at approximately 50 Ma, possibly leading to a time-transgressive transition from "flat-slab" to "steep-slab" subduction (Coney and Reynolds 1977; Engebretson et al. 1985). The southward sweep of volcanism across the Cordillera may track the progressive steepening and foundering of the subducting plate as the rate of plate convergence decreased through much of Tertiary time (Cross and Pilger 1978; Lipman 1980). Such a plate boundary evolution would favor extension by both relaxing contractional boundary conditions and thermally weakening the lithosphere as a hot asthenospheric wedge invaded the space opening be-

Manuscript received July 5, 2000; accepted August 14, 2001.

[1] Present address: Department of Geology and Geophysics, Yale University, P.O. Box 208109, New Haven, Connecticut 06520-8109, U.S.A.

[2] Author for correspondence; e-mail: Allen.McGrew@notes.udayton.edu.

[3] Department of Geological Sciences, The Ohio State University, Columbus, Ohio 43210, U.S.A.

[The Journal of Geology, 2002, volume 110, p. 179–194] 0022-1376/2002/11002-0004$15.00

tween the base of the overriding lithosphere and the downgoing slab (Best and Christiansen 1991). A similar process is proposed by Humphreys (1995), who argues that delamination of the shallowly subducting Farallon slab allowed for the upwelling of hot asthenosphere against the base of the lithosphere. Convective removal of thickened lithospheric mantle is another possible cause of Basin and Range extension (Platt and England 1994). Detachment of dense mantle lithosphere would lead to an influx of hot asthenospheric mantle that could trigger melting and cause regional uplift due to mantle buoyancy, thus providing potential energy for horizontal extension (Houseman et al. 1981; Platt and England 1994; Sonder and Jones 1999).

Distinguishing the relative contribution of the various mechanisms outlined above depends mostly on the answers to two questions: (1) Was the crust in a particularly overthickened condition at the onset of Paleogene extension? (2) What were the magnitude, kinematics, and timing of extensional systems relative to regional volcanism? Although the issues are simple, the resolution is difficult due to the complexity and patchiness of volcanism and extension in time and space on a regional scale (Axen et al. 1993). Consequently, the answers to these questions do not depend on relationships in any one area but must emerge from regional synthesis based on careful documentation of field relationships in numerous critical areas.

The timing and magnitude of the early phases of extension in the northern Basin and Range is crucial to orogen-wide models for the driving forces of regional extension (Sonder and Jones 1999). Nevertheless, regional Eocene extension in the northeastern Basin and Range has been widely suspected but only locally documented (Potter et al. 1995; Camilleri and Chamberlin 1997; Mueller et al. 1999). To address these problems, this article documents an early extensional fault system in the Copper Mountains, Nevada, a previously little-studied terrain in the northeastern Basin and Range province (figs. 1, 2). Because the Copper Mountains also preserve a history of Late Cretaceous shortening in the hinterland of the Sevier fold and thrust belt, they shed light on the fundamental tectonic transition from Late Cretaceous contraction to Tertiary extension. Significantly, the area also contains a well-studied Eocene flora that affords a rare opportunity to characterize Early Tertiary paleoelevation (Axelrod 1966; Povey et al. 1994; Wolfe et al. 1998). New geochronological and structural data presented here constrain the timing, magnitude, and kinematics of extension in the Copper Mountains with important implications for the causes and evolution of extension in the northern Basin and Range.

Pre-Tertiary Geologic History

The Copper Mountains and surrounding areas expose a sequence of Late Precambrian and Early Paleozoic metasedimentary rocks interpreted to record passive margin sedimentation. The Copper Mountains are composed of phyllite and quartzite of the Precambrian McCoy Creek Group and the overlying Cambrian Prospect Mountain Quartzite (Coats 1987). Above these units is the Ordovician Tennessee Mountain Formation, which consists of laminated and thinly bedded marble and siltstone with a minimum thickness of approximately 1600 m (Bushnell 1967).

These upper Proterozoic–lower Paleozoic metasedimentary rocks contain a phyllitic cleavage (S_1) commonly overprinted by a northeast-striking, steeply dipping crenulation cleavage (S_2) oriented parallel to the axial surfaces of northeast-trending outcrop-scale to map-scale folds. Field observations suggest that the second deformational event was synchronous with the intrusion of the Coffeepot Stock, a granodiorite body intruded during the late Cretaceous (McGrew et al. 2000*b*). The eastern part of the stock displays a weak solid-state grain shape foliation developed under greenschist facies conditions and striking parallel to the crenulation cleavage. Some dikes emanating from the eastern part of the stock are involved in folding, whereas others cut folds, implying that the stock must have been emplaced synkinematically with the second deformational event (McGrew et al. 2000*b*). The older cleavage (S_1) is constrained only to predate the emplacement of the Cretaceous stock, but similar deformation in the Mountain City area has been bracketed between Triassic and Late Jurassic (Little 1987). Tectonic burial and imbrication of the Late Proterozoic to Ordovician metasedimentary sequence may also date to this time period because the Coffeepot Stock cuts premetamorphic thrust faults north of Copper Mountain (McGrew et al. 2000*b*).

The Coffeepot Stock consists mostly of medium-grained hornblende biotite quartz monzonite. Locally, it contains distinctive cream-colored euhedral orthoclase phenocrysts up to 2.5 cm in size. Biotite and hornblende typically compose 5%–10% of the rock, although hornblende is not universally present. Accessory phases include euhedral apatite, sphene, allanite, and magnetite. Chlorite frequently appears as an alteration product of biotite,

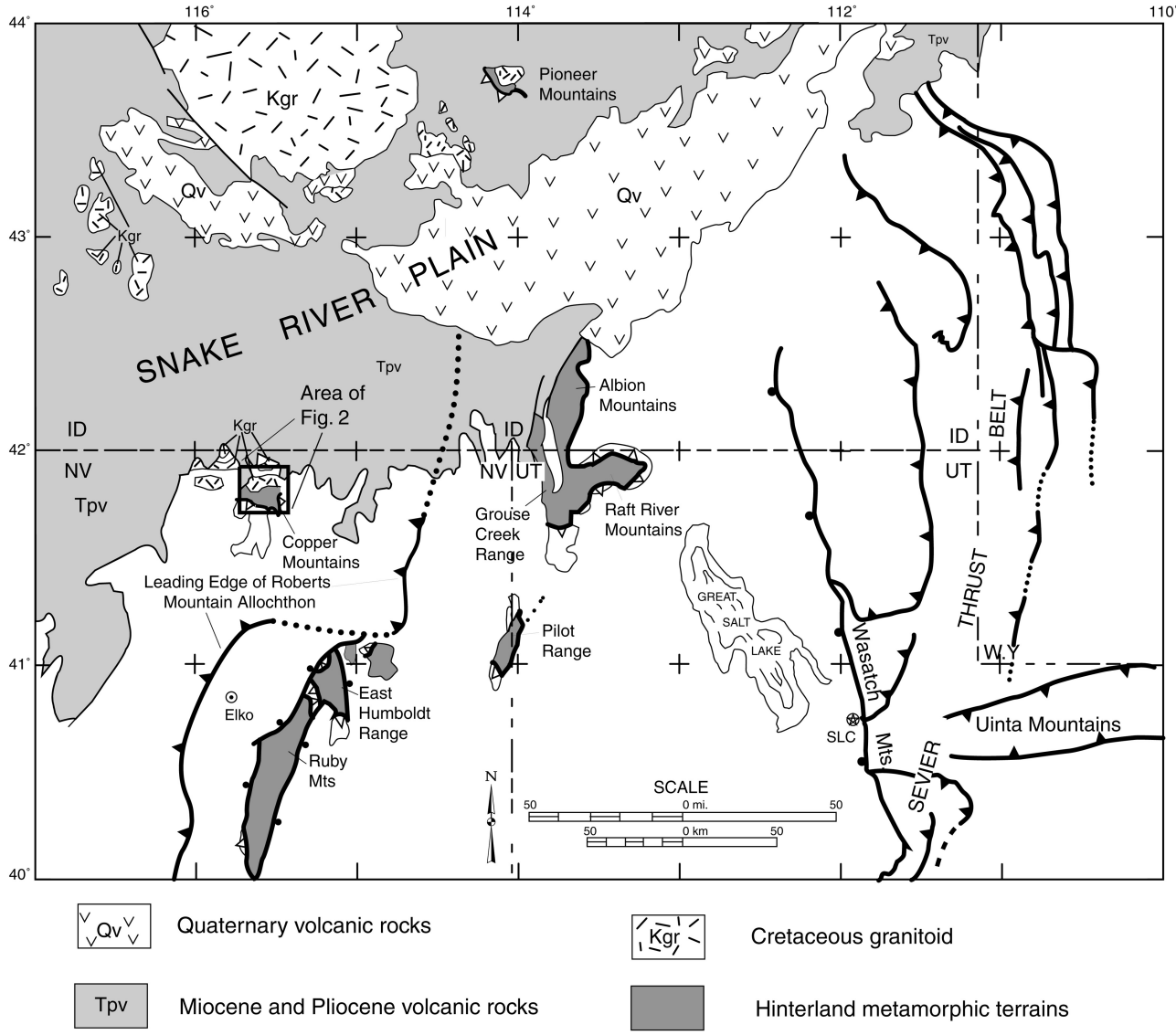

Figure 1. Generalized tectonic map of the northeastern Basin and Range province showing the Copper Mountains and other hinterland metamorphic terrains in relationship to major tectonic features. Heavy lines with solid triangles indicate the positions of major thrust systems: the Sevier thrust belt to the east and the leading edge of the Roberts Mountain allochthon in northeastern Nevada. Heavy lines with open triangles indicate major detachment fault systems, whereas heavy lines with solid circles indicate major high-angle normal fault systems.

and secondary epidote and white mica are also present locally. Feldspar is usually at least partially sericitized. Numerous small, late-stage aplitic and pegmatitic dikes cut the pluton. In immediate proximity to the stock, the Tennessee Mountain Formation has been metasomatized to form a distinctive, 3–4-m-thick garnet-epidote skarn. Locally, andalusite and staurolite appear to be pre- or synkinematic with respect to phyllitic cleavage, but andalusite also grew postkinematically to phyllitic cleavage in the contact aureole of the Cretaceous pluton.

The depth of burial of the above terrain is approximately constrained by plutonic and metamorphic relationships. The Coffeepot Stock evinces a generally mesozonal character, with relatively coarse grain size even near its margins and a broad contact aureole that merges distally into regionally metamorphosed rocks. The presence of andalusite in the contact aureole of the stock re-

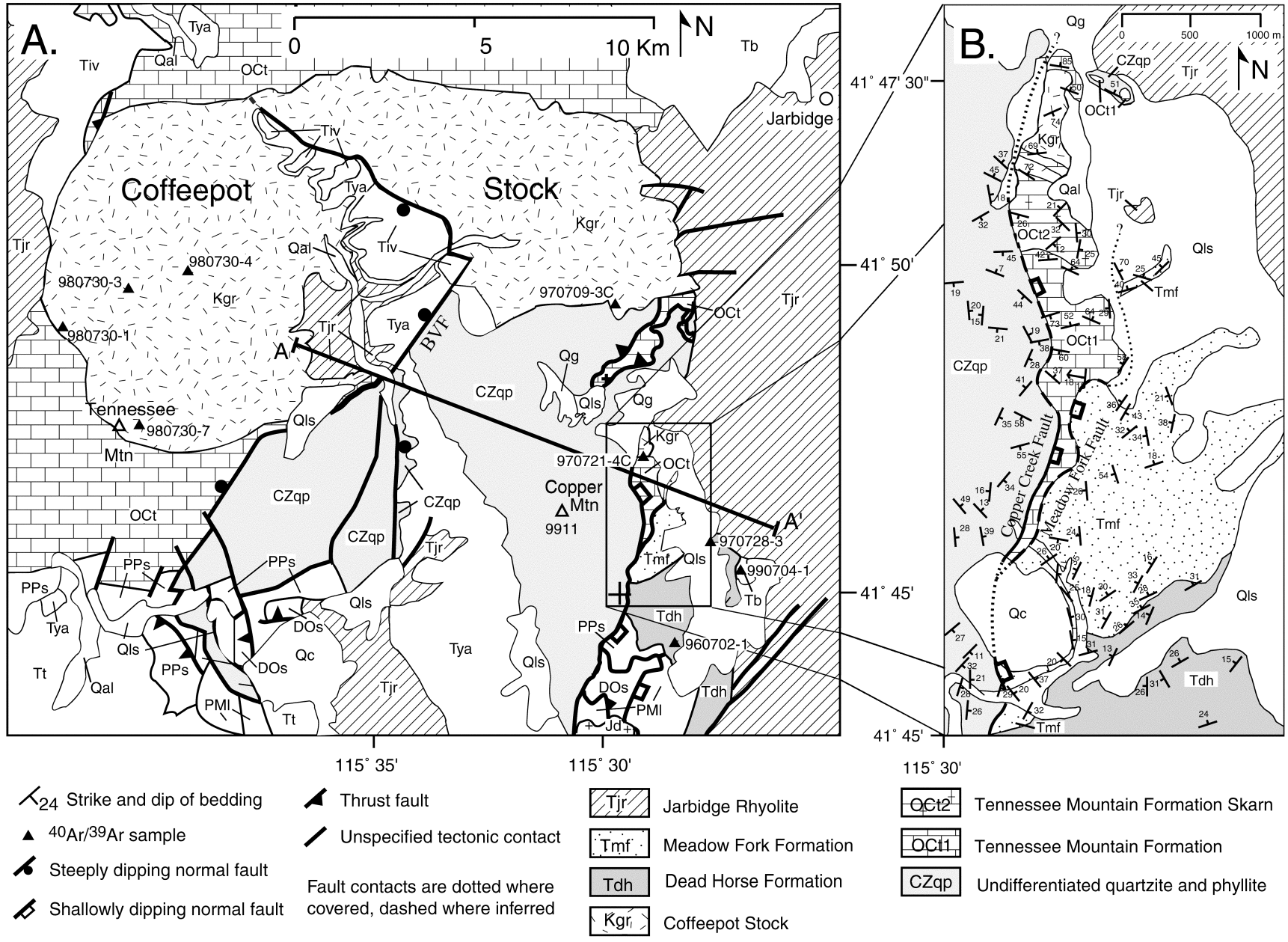

quires peak metamorphic pressures of <3.75 kb (Holdaway 1971), equivalent to burial depths of less than ~14 km. Conversely, fibrolitic sillimanite found in the presence of muscovite in the immediate contact zone of the deeper-seated eastern part of the pluton indicates minimum pressures of at least 2.2 kb according to the bathozone scheme of Carmichael (1978). The absence of cordierite in the contact aureole further supports this minimum pressure estimate, as does the widespread occurrence of stable hornblende in the granitoid, suggesting that fluid pressure (and therefore total pressure) was probably not <2 kb, assuming that water content was greater than ~3.5% (Naney 1983). Taken together, these relationships suggest that the pluton intruded at depths of at least 8 km but no more than 14 km.

The history of crustal shortening that led to tectonic burial of this terrain is a matter of continuing debate (cf. Coats and Riva 1983; Ketner et al. 1993; Ketner 1998), but it is clear that, before Tertiary extension, a stack of thrust sheets related to Paleozoic and Mesozoic contraction overlay the entire area. These units have since been tectonically and erosionally removed, and Late Eocene tuffs unconformably overlie all of the above structural and stratigraphic features.

Geology of Copper Basin

The Copper Mountains are bounded to the east by two east-dipping low-angle normal faults that drop down the Copper Basin fault block to the east (fig. 2*B*). The westernmost of these faults, the Copper Creek Fault, is excellently exposed along Copper Creek on the southeastern flank of Copper Mountain, where it is oriented 020°, 30°. In this area, the fault separates the Late Eocene Dead Horse Formation above from the Late Proterozoic to Cambrian quartzite and phyllite sequence below. The fault itself is conspicuously marked by a ledge of extremely fine-grained, flinty-textured quartzite mylonite approximately 1–2 m thick. Petrographic observation of the fault rock reveals an extremely homogeneous mass of fine, polygonal quartz grains with a mean grain size of <10 μ. Overprinting the early history of ductile strain is a later history of brittle deformation, documenting the ductile-through-brittle evolution of the fault system. The fault surface is locally brecciated and contains slip lineations with an average orientation of 22°, 131° (fig. 3) and meter-scale swales with a trend ~135°. These features indicate that movement on the Copper Creek Fault was mostly dip slip toward the southeast. Although the fault currently dips 25°–30° southeastward, a package of Tertiary sedimentary and volcanic rocks in the hanging wall dips 20°–30° northwestward (fig. 4). Thus, assuming the hanging-wall strata were horizontal before faulting, the initial dip of the faults must have been 45°–60° SE. Although the faults could not have cut through the upper crust at an initially low angle, their inclination could have decreased listrically at depth.

In the northern part of Copper Basin, a fault slice of intensely deformed, fine-grained marble and calcareous phyllite intervenes between the quartzite and phyllite sequence to the west and the Tertiary volcanic-sedimentary sequence to the east. The western contact of this fault slice is interpreted as the northward continuation of the Copper Creek Fault, whereas the eastern contact is a splay off the Copper Creek Fault, here named the "Meadow Fork Fault" (fig. 2*B*). The marble/phyllite sequence in the intervening fault slice is intruded by a small body of quartz monzonite, and the contact aureole is marked by a well-developed skarn, contact relationships similar to those of the Coffeepot Stock farther west. Since the quartz monzonite is older than the Copper Creek Fault and does not intrude the footwall of the fault in this area, the Copper Creek Fault probably transported it to its current location.

All available evidence supports the hypothesis that this fault slice correlates with rocks exposed in the footwall of the Copper Creek Fault near Ten-

Figure 2. Generalized geologic map of the Copper Mountains area showing sample localities referred to in this study (modified from Coats 1987). *BVF* = Bruneau Valley Fault; *CZqp* = Late Proterozoic and Lower Cambrian quartzite and phyllite, undifferentiated (includes McCoy Creek Group and Prospect Mountain Quartzite); *OCt*1 = Upper Cambrian to Ordovician Tennessee Mountain Formation; *OCt*2 = Skarn, interpreted as metamorphosed Tennessee Mountain Formation; *DOs* = Ordovician to Devonian dolostone; *PPs* = Pennsylvanian to Permian Sunflower Formation; *PMh* = Mississippian to Permian Havallah sequence; *Jd* = Jurassic diorite; *Kgr* = Cretaceous granitoids of the Coffeepot suite (ranging from quartz monzodiorite to granite); *Tb* = Tertiary basalt; *Tdh* = Late Eocene Dead Horse Formation and interbedded lacustrine strata and coarse clastic rocks; *Tmf* = Late Eocene to Early Oligocene Meadow Fork Formation conglomerate; *Tjr* = Miocene Jarbidge Rhyolite; *Tya* = Miocene Young America Gravel; *Qls* = Quaternary landslide deposits; *Qal* = Quaternary alluvium; *Qc* = Quaternary colluvium.

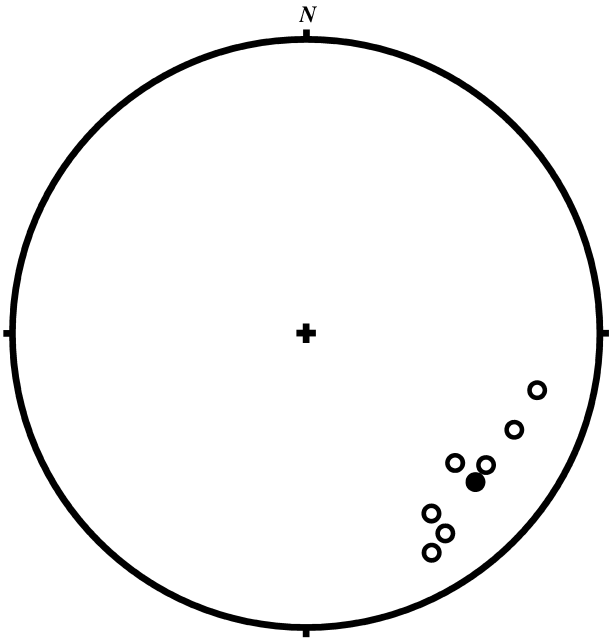

Figure 3. Equal area lower hemisphere projection of slip lineation orientations on the Copper Creek normal fault; mean = 22°, 131° (*solid circle*); $N = 7$.

nessee Mountain approximately 10 km NW. The lithology and deformational style of the fine-grained marble and calcareous phyllite of the Copper Basin fault slice closely resemble the Tennessee Mountain Formation to the west. Both localities show early cleavages that were overprinted later by folding. In addition, the field relationships and mineralogy of the skarn exposed in the Copper Basin fault slice is remarkably similar to the skarn observed near Tennessee Mountain. Both assemblages are dominated by massive grossular-andradite garnet with associated epidote, diopside, hornblende, and calcite as well as the ore minerals scheelite, molybdenite, and powellite (Lapointe et al. 1991). Also, both areas are cut by northwest-striking quartz veins. Moreover, as described below, the plutonic rocks of the Copper Basin fault slice are similar in age to the Coffeepot Stock.

The lower part of the sequence of Tertiary volcanic and sedimentary rocks that overlie the Copper Creek and Meadow Fork faults consists of the Dead Horse Formation, an approximately 1600-m-thick package of crystal-vitric and pumiceous tuffs and tuffaceous sediments. The composition of the tuffs ranges from biotite-hornblende dacite to biotite-hornblende quartz latite to biotite rhyolite tuff (Coats 1964). This unit dips northwestward with an average orientation of 217°, 22° (fig. 4). South of Copper Basin, this unit rests unconformably on Paleozoic limestone, which is also in the hanging wall of the Copper Creek Fault (fig. 2*A*). The lower part of the Dead Horse Formation consists predominantly of massive devitrified welded tuff ranging from pale gray to pale brown, white or green in color. The proportion of sedimentary rocks increases upward through the formation.

The upper part of the Dead Horse Formation ranges from tuffaceous shale (lake beds) to tuffaceous arkose and pebble-cobble conglomerate, all interbedded with white airfall tuffs. The ashy lacustrine shales contain abundant fossilized plants representing a Late Eocene temperate, mixed conifer-deciduous hardwood flora that lived near a lake formed in a narrow, northeast-trending, fault-bounded basin (Axelrod 1966). Tuff layers are interspersed throughout but become less dominant upward through the sequence. Poorly sorted, matrix-supported pebble and boulder conglomerates interpreted as debris flows become more conspicuous near the top of the section and are dominant in the overlying Meadow Fork Formation.

The Dead Horse Formation grades conformably upward into the Meadow Fork Formation, a poorly sorted, poorly bedded, matrix-supported conglomerate containing clasts of quartzite, marble, phyllite, skarn, and abundant granitoid boulders up to 1 m in diameter. Bedding is massive, and sedimentary structures, such as pebble imbrication and cross-bedding, are generally absent although channel cuts filled with grain-supported conglomerate are present locally. The granitoid boulders are commonly spheroidal, but most other clasts are angular to subangular. Volcanic tuffs are present locally but are much less abundant than in the underlying Dead Horse Formation. The average orientation of the Meadow Fork Formation is 216°, 21°, nearly identical to the underlying Dead Horse Formation (fig. 4). The Meadow Fork Formation is not fossiliferous and is only constrained to be younger than the uppermost Dead Horse Formation and older than the Seventy-Six Creek Basalt, which overlies it with angular unconformity.

The stratigraphic architecture outlined above and the presence of sparse metamorphosed footwall clasts indicate that extension on the Copper Basin fault system probably began during deposition of the upper part of the Dead Horse Formation. The bulk of extension probably postdates eruption of the basal tuffs of the Dead Horse Formation for two reasons. First, the Dead Horse Formation is not rotated significantly more than the overlying Meadow Fork Formation (fig. 4). Second, the pebbly horizons in the upper part of the Dead Horse For-

mation contain few clasts of lower plate lithologies, such as marble, quartzite, phyllite, and granitoid. Instead, the Dead Horse Formation contains abundant clasts of sedimentary rocks, especially argillite, chert, and carbonate similar to the Paleozoic rocks on which it was deposited. In contrast, lower plate clasts (especially granitoid) become dominant in the overlying Meadow Fork Formation. It appears that during deposition of the upper Dead Horse Formation, tectonic unroofing had not yet proceeded to the extent recorded by the overlying Meadow Fork Formation. Consequently, the lacustrine strata and interbedded pebbly horizons in the upper Dead Horse Formation probably record only the initial phases of extension. Significantly, the outcrop area of the Meadow Fork Formation is now separated from the nearest extensive outcrops of the Coffeepot Stock by several kilometers, suggesting that the Meadow Fork Formation was translated several kilometers to the southeast after deposition and that the Copper Mountains were later uplifted in between. The Copper Creek and Meadow Fork normal faults provide the only structures of suitable age and kinematics to cause this translation.

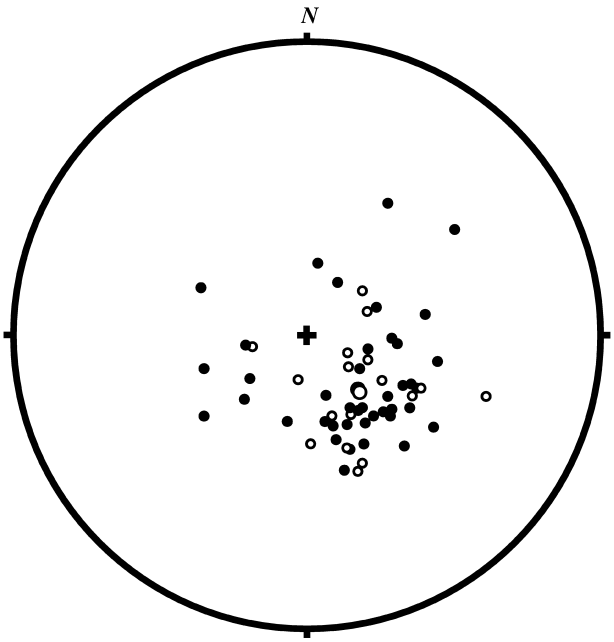

Figure 4. Equal area lower hemisphere projection of poles to bedding in the sedimentary and volcanic sequence of the hanging wall of the Copper Creek and Meadow Fork normal fault system. *Open circles* = Dead Horse Formation: $N = 17$; mean = 217°, 22°. *Solid circles* = Meadow Fork Formation: $N = 42$; mean = 216°, 21°. Mean orientations are shown by larger diameter circles.

$^{40}Ar/^{39}Ar$ Thermochronology

In order to better constrain the emplacement and cooling history of the Coffeepot Stock and the age of the Tertiary volcanic and sedimentary sequences, incremental-heating $^{40}Ar/^{39}Ar$ age measurements were performed on separated minerals from a suite of samples from the Copper Mountains area. The results are summarized in table 1 and shown in figure 5. Full details, including a discussion of analytical methods, are available from *The Journal of Geology*'s Data Depository upon request.

The discussion here is based on customary age spectra. Table 1 also presents the results of the isotope correlation approach, but these results are not further discussed because they generally reinforce the interpretations of the age spectra but do not provide additional insights. Except for a few, generally small, low- and very high-temperature fractions, the spectra are internally concordant or show only restricted discordance. Half of the mineral separates yield plateaus under strict definition (see table 1), and for these samples, the term "age" used below implies a plateau age. The remainder of the samples display some discordance, but all still have broad "plateau" regions covering most of the Ar release; over these regions, variations in apparent age exceed somewhat those expected from analytical uncertainties alone, but this discordance is relatively minor. In these cases, "approximate plateau ages" are defined. In general, this minor discordance is attributed to impurities and alteration with concomitant ^{39}Ar recoil effects consistent with observed concomitant K/Ca variations and petrography. Although less confidence is attached to the approximate plateau ages, they also are interpreted to carry geological significance.

Cooling History of the Coffeepot Stock. For the Coffeepot Stock (table 1; figs. 2*A*, 5*A*–5*I*) hornblende yields ages ranging from 103.7 to 106.8 Ma. Except for sample 970709-3C, which is discussed below, biotite yields ages that are consistently somewhat younger than the corresponding hornblende ages ranging from 99.2 to 104.7 Ma. Among all these mineral specimens, biotite samples 980730-3 and 980730-7 show the most significant internal discordance (fig. 5*D*, 5*F*). Both show similar spectra consisting of approximate plateaus broken in the middle by depressed apparent ages for the 800°–1000°C temperature increments. Concomitant K/Ca variations suggest that these fractions reflect release of ^{39}Ar recoiled into a relatively

Table 1. Summary of $^{40}Ar/^{39}Ar$ Analytical Results

Sample	Material	Run (no.)	K (wt %)[a]	t_{int}[b]	Age spectrum		Isotope correlation		
					t_p[c]	(% ^{39}Ar)[d]	t_{ic}[e]	MSWD[f]	Intercept[g]
980730-1	Hornblende	63B40	.67	105.0	105.1 ± .3	96	105.2 ± .3	5, 1	291 ± 9
980730-1	Biotite	63B39	7.5	100.9	"101.4 ± .3"	89	101.4 ± .3	3, 9	299 ± 7
980730-3	Hornblende	63B51	.80	101.5	"103.7 ± .4"	89	103.2 ± .4	4, 4	301 ± 5
980730-3	Biotite	63B41	6.8	97.5	"99.2 ± 1.2"	84	101.4 ± .7	40, 8	284 ± 10
980730-4	Biotite	63B43	7.5	101.1	102.3 ± .3	91	102.4 ± .3	2, 4	295 ± 4
980730-7	Biotite	63B44	7.1	101.8	"103.3 ± .4"	85	103.6 ± .4	14, 8	302 ± 12
970721-4C	Hornblende	60C6	.72	107.2	106.8 ± .4	89	106.6 ± .5	12, 5	327 ± 20
970721-4C	Biotite	60C4	8.1	104.6	104.7 ± .3	58	105.2 ± .3	9, 3	293 ± 12
970709-3C	Biotite	60C2	8.2	91.8	"93.0 ± .3"	88	93.2 ± .3	12, 3	290 ± 13
960702-1A	Biotite	55C22	7.4	40.0	41.3 ± .1	70	40.9 ± .2	5, 6	302 ± 3
970728-3	Sanidine	60C13	4.3	37.9	37.4 ± .2	95	37.8 ± .2	1, 2	284 ± 10
990704-1	Plagioclase	66C17	.32	16.3	16.5 ± .2	83	16.3 ± .1	4, 4	298 ± 2

Note. Analytical measurements performed in the Radiogenic Isotopes Laboratory at The Ohio State University. See supplemental data (available from *The Journal of Geology*'s Data Depository upon request) for procedural information, a full listing of analytical data, and plots of all data. The monitor used was an intralaboratory muscovite standard ("PM-1") with an $^{40}Ar/^{39}Ar$ age of 165.3 Ma. The age for this monitor was determined by simultaneous cross calibration with several monitors including the Fish Canyon Tuff biotite standard (FCT-3) with an age of 27.84 Ma. A systematic uncertainty of 1% is assigned to all ages in order to allow for uncertainties in the standards against which PM-1 was calibrated; this uncertainty is not included in the uncertainties given.

[a] Weight percentage of potassium in the bulk separate determined by the total quantity of ^{39}Ar produced during neutron irradiation and released during incremental-heating analysis.

[b] Integrated (or total-gas) age in Ma derived from the summation of all fractions of the incremental-heating analysis.

[c] Plateau age in Ma, with 1σ uncertainty, derived from the incremental-heating spectrum.

[d] Percentage of total ^{39}Ar in the plateau fractions. A "plateau" is defined as contiguous fractions constituting a majority of the ^{39}Ar released where the apparent-age variations among fractions may be accounted for with analytical uncertainties. A plateau encompasses as many fractions as possible (except where fraction uncertainties are very large) where ages agree with the plateau within their $\pm 2\sigma$ uncertainties. Where this strict definition is not observed and variation among plateau fractions is minor but still exceeds analytical uncertainties, an approximate plateau is defined (see fig. 6). In these cases, the indicated plateau age is enclosed in quotation marks.

[e] Isotope-correlation age (in Ma), with 1σ uncertainty, derived from the $^{36}Ar/^{40}Ar$ versus $^{39}Ar/^{40}Ar$ regression, with a few severely discordant fractions omitted.

[f] Mean square weighted deviation of the regression analysis where the second number is the number of deleted fractions.

[g] $^{40}Ar/^{36}Ar$ ratio (with 1σ uncertainty) for the indicated nonradiogenic component.

calcic inclusion phase. Petrographically, these rock samples are slightly deformed and show limited secondary alteration involving the partial replacement of biotite by chlorite and/or epidote along laminae parallel to the basal plane. In addition, sphene and, less commonly, apatite are present locally as inclusions in biotite. Breakdown of any of these phases could produce the inferred recoil effects, thus explaining the modest discordance of these spectra.

Except for the limited secondary alteration effects described above, the western part of the pluton shows no evidence of postemplacement metamorphism. Accordingly, the above ages are interpreted to record cooling following emplacement of the pluton. Two samples from the western part of the pluton (980730-1 and 980730-3) yield ages for both hornblende (105.1 and 103.7 Ma) and biotite (101.4 and 99.2 Ma; fig. 5*A*–5*D*). The age difference in both cases is ~4 m.yr. Assuming hornblende and biotite closure temperatures of 500° and 300°C, respectively, the apparent cooling rate was ~50°C/m.yr. Furthermore, assuming a solidus temperature of ~700°C and a constant cooling rate suggests that the pluton crystallized at ~108–109 Ma.

Sample 970721-4C from a small body of granite in the Copper Basin fault slice yields slightly older plateau ages (fig. 5*G*, 5*H*) for both hornblende (106.8 Ma) and biotite (104.7 Ma) for a difference of ~2 m.yr. Using the same assumptions as above, these ages imply a significantly higher cooling rate of ~100°C/m.yr. but a similar crystallization age of ~109 Ma. Thus, the granitoid of the Copper Basin fault slice probably crystallized at the same time, or nearly so, as the Coffeepot Stock. In addition, the slightly older cooling ages and the higher rate of cooling are consistent with the hypothesis that this fault slice is an allochthonous piece of the upper part of the Coffeepot Stock. In the tectonic reconstruction favored below, this fault slice would originally have overlain the western part of the pluton.

Biotite sample 970709-3C from the eastern part of the Coffeepot Stock yields a somewhat discordant spectrum with an approximate plateau age of 93.0 ± 0.3 Ma for a broad region covering 88% of

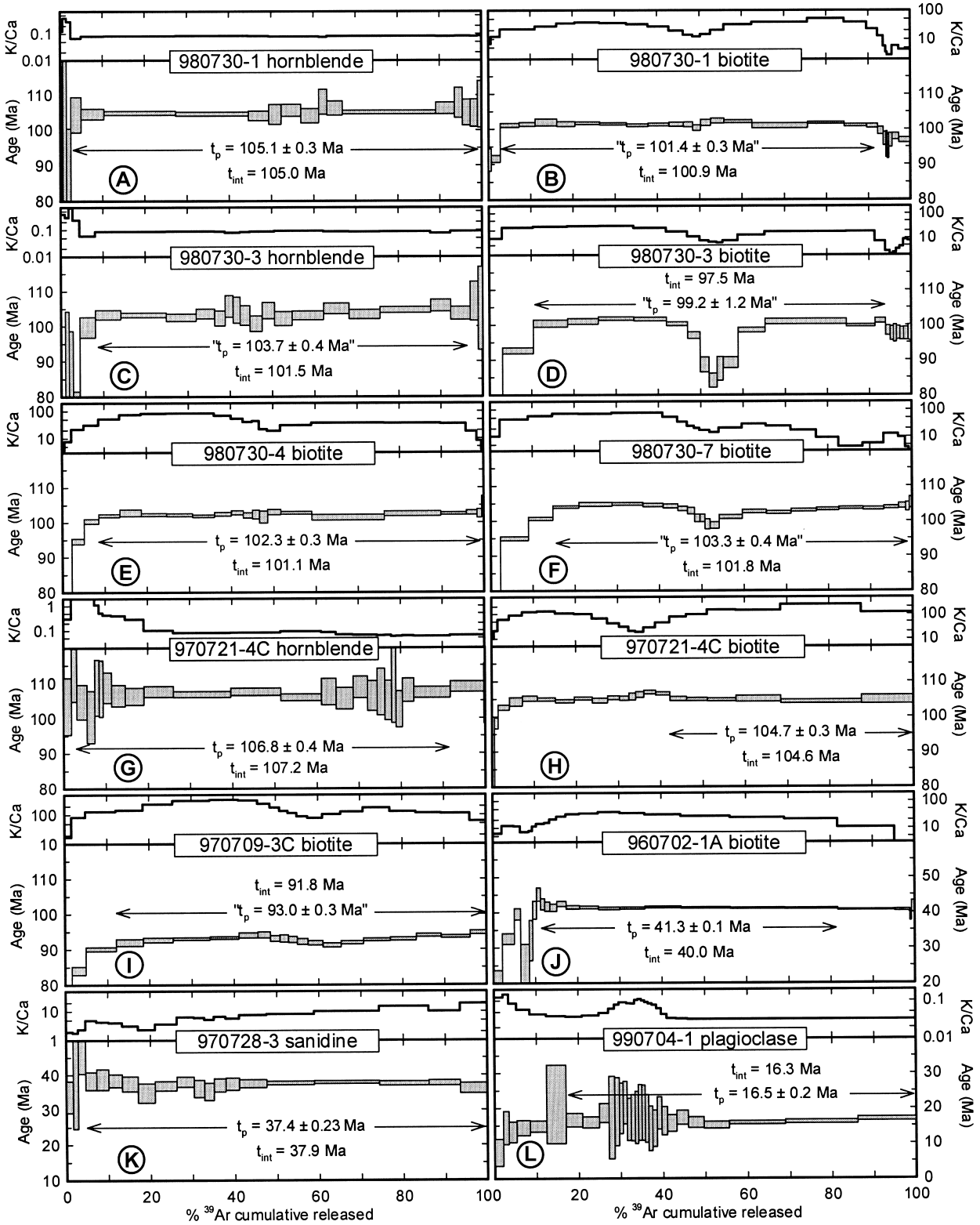

Figure 5. $^{40}Ar/^{39}Ar$ age spectra. t_{int} = integrated age from combining all fractions weighted by the amounts of ^{39}Ar; t_p = plateau age. The presence of quotation marks signify that the scatter on the indicated fractions somewhat exceed that expected from purely analytical errors. Age uncertainties are shown at the 2σ level.

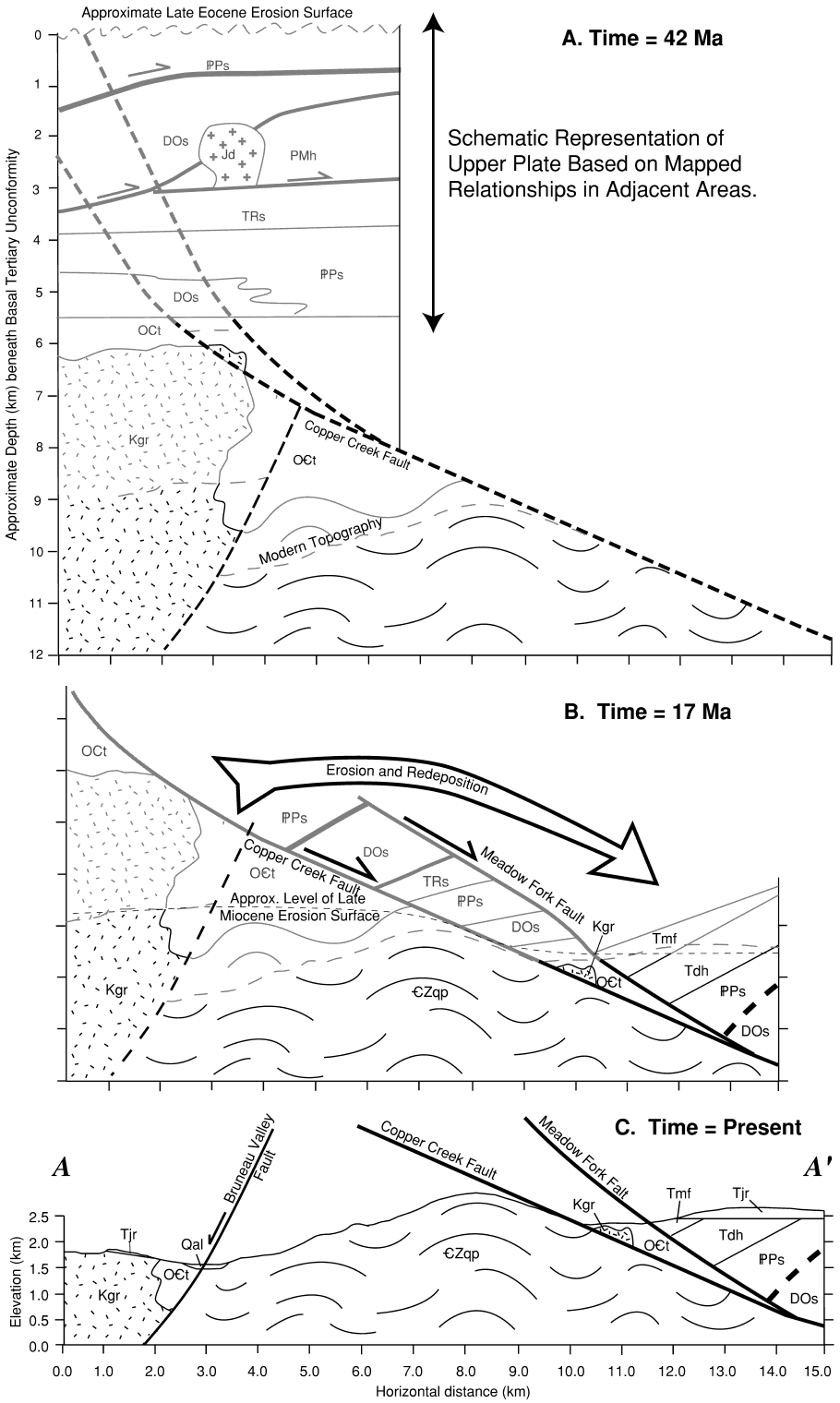

Figure 6. Retrodeformed cross section sequence for the Copper Basin fault system along line *A*-*A′* in figure 2. *A*, Initial state immediately before the onset of extension at ~42 Ma. Due to extensive cover and poorly known or ambiguous contact relationships, structural levels above the Tennessee Mountain Formation are illustrated schematically. However, unit thicknesses and structural relationships are consistent with relationships in adjoining areas (e.g., Coats 1964, 1987; Bushnell 1967; Coash 1967; Ketner et al. 1993, 1995). The restored position of the modern

the ^{39}Ar released where apparent ages range only from ~92–95 Ma (fig. 5*I*). Although a strict plateau is not observed, this biotite clearly gives a younger age than the biotites discussed above from the western part of the pluton (fig. 2*A*). Petrographically, this sample displays a well-defined foliation and much more extensive secondary alteration than those from the western part of the pluton. Sericitic alteration is abundant, and biotites are commonly mottled in appearance and more extensively replaced by chlorite and epidote, raising the possibility that the 93-Ma age records cooling following metamorphism rather than simple conductive cooling following emplacement of the granitoid. This suggests that the eastern part of the pluton may have intruded deeper levels and cooled more slowly than the western part of the pluton. This interpretation is consistent with the observation that the eastern part of the pluton intrudes deeper stratigraphic levels and carries a solid-state foliation and a greenschist facies overprint that is less evident to the west. In addition, the eastern part of the pluton occupies the footwall of the Miocene-aged Bruneau Valley normal fault system (fig. 2*A*) and so would be expected to restore back to deeper structural levels than the western part of the pluton according to the tectonic reconstruction developed below.

Age Relationships in Tertiary Volcanic/Sedimentary Sequence. Two samples from the Dead Horse Formation yield ^{40}Ar/^{39}Ar results that bracket the age of the Dead Horse Formation and therefore the initiation of the Copper Basin fault system. Strongly oxidized biotite from near the base of the Dead Horse Formation yields a somewhat disturbed spectrum that nevertheless defines a plateau age of 41.3 ± 0.1 Ma over most of the ^{39}Ar released (figs. 2*A*, 5*J*). This rock consists of welded, dark olive green ash-flow tuff with abundant phenocrysts of oxidized biotite and plagioclase in the oligoclase/andesine range. A sanidine age of 37.4 ± 0.2 Ma comes from a sample of white airfall tuff from the uppermost part of the Dead Horse Formation, thereby constraining the age of one of the final pulses of Late Eocene volcanism (figs. 2*A*, 5*K*). In addition to sanidine, this rock also contains abundant phenocrysts of plagioclase and quartz and sparse phenocrysts of biotite and hornblende, the latter occurring mostly in pumice fragments. The groundmass is glassy and contains abundant bubble-wall shards. K/Ca ratios and K are lower than expected for sanidine, so it is likely that a small amount of plagioclase (± quartz) are included in the sanidine separate. The fossiliferous lake beds described by Axelrod (1966) lie between the two dated horizons, thus bracketing the age of lacustrine deposition. Since the lake beds and the associated coarse clastic strata are interpreted to be early syntectonic with respect to an evolving fault-bounded basin, this implies that the Copper Creek–Meadow Fork normal fault system also formed between 41.3 and 37.4 Ma.

The Copper Creek/Meadow Fork Fault system ceased to be active before eruption of the Seventy-Six Creek Basalt and the overlying Jarbidge volcanic sequence. The Seventy-Six Creek Basalt yields an ^{40}Ar/^{39}Ar plagioclase age of 16.5 ± 0.2 Ma (fig. 5*L*), providing a minimum age for the cessation of faulting. However, due to the inferred high sedimentation rate and the conformable nature of its basal contact, the Meadow Fork Formation is inferred to be latest Eocene or Early Oligocene in age.

Extensional Fault Reconstruction

The history of faulting in the Copper Mountains is summarized in figure 6. The initial geometry at ~42 Ma is illustrated by figure 6*A*. Before the onset of extension, the Upper Proterozoic and Lower Paleozoic sediments had been metamorphosed, foliated and folded at least twice, tectonically buried beneath thrust sheets of western facies and Havallah sequence rocks, and intruded by the Coffeepot Stock. Metamorphic phase relationships in the contact aureole of the Coffeepot Stock indicate that it intruded at pressures of 2.2–3.75 kb, equivalent to depths of 8–14 km. In addition, a thrust-thickened package of sedimentary rocks as young as Triassic occupies the hanging wall of the Copper Creek Fault system and must restore back to a position overlying the Copper Mountains area when Ter-

erosional surface is indicated by a shaded dashed line, and all units above this line are also shaded. *B*, Cross section after displacement on the Copper Creek and Meadow Fork normal faults but immediately before activity on the Bruneau Valley normal fault system. Levels above the restored position of the modern erosional surface are again shaded. The approximate level of the Late Miocene erosional surface is shown by a fine broken line. *C*, Modern cross section established after eruption of the Jarbidge Rhyolite and down-faulting of the western fault block on the Bruneau Valley normal fault system.

tiary extension is removed (see below). In sum, the lower plate of the Copper Creek Fault system was probably exhumed from paleodepths of ~11 ± 3 km.

Normal faulting began between 41.3 and 37.4 Ma during the final stages of a major episode of tuffaceous volcanism represented by the Dead Horse Formation. As the fault block moved southeastward, it generated significant topographic relief that resulted in the erosion of footwall rocks and their subsequent incorporation into the Meadow Fork Conglomerate. The dominance of granitoid clasts in the Meadow Fork Formation suggests that at the time of deposition, the Meadow Fork basin was much closer to the Coffeepot Stock than at present, and subsequent displacement translated it progressively toward the southeast (fig. 6*B*).

The Copper Basin fault slice is inferred to be an allochthonous slice of the Coffeepot Stock and its country rock, the Tennessee Mountain Formation, which is exposed approximately 10 km to the west-northwest of Copper Basin. Therefore, the intrusion provides a cutoff constraining the apparent displacement on the fault. Map relationships require that movement on the Copper Creek normal fault was a minimum of 8 km, possibly up to 12 km or more, in a southeasterly direction. Displacement on the overlying Meadow Fork Fault is not constrained but must be of comparable magnitude in order to juxtapose the Tertiary volcanic and sedimentary sequence down against the metamorphosed strata and associated plutonic rocks of the Copper Basin fault slice.

These data also constrain the age of faulting. Field relationships require that faulting postdates the Cretaceous Coffeepot Stock and predates the 16.5-Ma Seventy-Six Creek Basalt and the overlying Jarbidge Rhyolite, which is deposited unconformably on both the hanging-wall and footwall blocks. In addition, abundant lower plate clasts in the Meadow Fork Conglomerate indicate that the footwall rocks had been exhumed to the surface by the time of Meadow Fork deposition. Moreover, the conformable contact between the Dead Horse Formation and the Meadow Fork Conglomerate suggests that significant extension began during the final stages of tuffaceous volcanism and continued after volcanism ceased. Lake and conglomeratic deposits in the upper part of the Dead Horse Formation also suggest the formation of a north-trending, fault-bounded basin (Axelrod 1966), and $^{40}Ar/^{39}Ar$ results bracket the age of that basin between 41.3 and 37.4 Ma.

Along the Bruneau Valley west of the Copper Mountains, the Jarbidge Rhyolite is itself cut by a complex network of steep, north-to-northeast-trending normal faults and rotated to dips of 10°–20° SE (figs. 2*A*, 6*C*). Overlying the Jarbidge Rhyolite in the Bruneau Valley is a thin sheet of conglomerate, the Young America Gravel (Bushnell 1967), that is, in turn, overlain by the Idavada Volcanics (Malde and Powers 1962). The Young America Gravel consists of angular to subrounded cobbles and boulders of quartzite and rhyolite 2 cm–1 m in diameter, suggestive of a syntectonic deposit. In addition, the outcrop pattern of the Young America Gravel and the Idavada Volcanics appears to be largely fault controlled along the Bruneau Valley. Nevertheless, the Young America Gravel and the Idavada Volcanics are rotated less than the underlying Jarbidge Rhyolite. The Idavada Volcanics in the Bruneau Valley have not been directly dated but are thought to be Late Miocene (Coats 1987), and the Bruneau Valley fault system is probably the same age.

Displacement on the Bruneau Valley fault system is probably not strictly dip slip because it appears that the southern margin of the Coffeepot Stock may have been translated up to 2 km toward the southwest, thus introducing a limited uncertainty into cross section reconstruction due to a small component of out-of-the-plane motion. For the purposes of cross section reconstruction, the vertical throw on the Bruneau Valley fault system is estimated to be ~2 km based on restoration of the base of the Jarbidge Rhyolite to a similar level as the flat-lying exposures of Jarbidge Rhyolite on the east side of the Copper Mountains. Following cessation of Miocene volcanism and activity on the Bruneau Valley fault system, erosion leads to the modern cross section (fig. 6*C*).

Discussion

Data from the Copper Mountains are consistent with several regional geologic patterns observed throughout the northeastern Basin and Range province. The age and lithology of the Dead Horse Formation correlates well with the northeastern Nevada volcanic field of Brooks et al. (1995), extending this volcanic province to the Copper Mountains and nearby areas. As indicated by Brooks et al. (1995), widespread siliceous volcanism permeated northeastern Nevada during Late Eocene time. Notably, this volcanism is similar in style and composition but slightly younger in age than the Challis volcanics extensively exposed in Idaho on the northern side of the Snake River Plain (Janecke and Snee 1993; Janecke et al. 1997).

Although slightly younger, the style of faulting

and basin development in the Copper Mountains resembles that observed north of the Snake River Plain. Janecke (1994) describes several extensional basins developed in east-central Idaho, each containing tuffs and conglomerates that overlie pre-Tertiary units. The extension in Idaho began between 46 and 48 Ma during the waning stages of Challis volcanism and continued until approximately 20 Ma (Janecke 1994; Janecke et al. 1997). The similarity in geologic framework between the Copper Mountains and the extensional province of east-central Idaho suggests a genetic link and forges a new connection across the Snake River Plain.

A southward sweep of volcanism along the length of the Cordillera has been documented by many studies (Armstrong 1970; Lipman et al. 1972; Gans et al. 1989; Armstrong and Ward 1991; Axen et al. 1993), and the data presented here reinforce this pattern. A number of workers argue for a strong correlation between the onset of volcanism and the onset of regional extension (e.g., Gans et al. 1989; Armstrong and Ward 1991), but others see a much weaker or no correlation (e.g., Best and Christiansen 1991; Axen et al. 1993; Janecke 1994). As noted by Axen et al. (1993), the divergent views in part reflect a problem of scale. For example, Armstrong and Ward (1991) identified large-scale correlations between extension and magmatism on the scale of the whole Cordillera based on 10-million-year time frames and regions hundreds of kilometers wide. In contrast, Janecke (1994) focused primarily on east-central Idaho and adjacent areas and recognized no southward progression of extension at that scale.

In the Copper Mountains, peak volcanism is concomitant with the onset of extension. The extensional basins of Janecke (1994) to the north in Idaho and of Gans et al. (1989) to the south in east-central Nevada follow a similar pattern, and the extension in the Copper Mountains appears to fill the gap between them, both spatially and temporally. Although Janecke (1994) has shown that the precise timing of extension does not progress southward through Idaho, the general pattern of volcanism and extension sweeping southward through time still appears to hold when the dates for the onset of extension at each latitude are compared on the scale of the entire Cordillera. Eocene extension began in British Columbia and Washington by ~52 Ma (Parrish et al. 1988), followed by Middle Eocene extension in Idaho (beginning ~50–46 Ma; Janecke 1994; Foster and Fanning 1997), and Late Eocene extension in northeastern Nevada according to this study. The onset of extension farther south in east-central Nevada was still younger (~37–35 Ma; Gans et al. 1989, 2001). This apparent southward progression of extension in sync with volcanism supports the idea that thermal weakening of the lithosphere was a crucial trigger mechanism for the onset of mid-Tertiary extension. In contrast, if gravitational potential energy stored in thickened continental crust was the primary driving force for extension, then there would be no reason to expect a geographic progression in the timing of the initiation of extension or correlation with the onset of volcanism.

Consequently, it is important to consider whether the timing of extension relative to volcanism in the Copper Mountains is truly representative of the northeastern Basin and Range province in general. Several workers have identified early phases of cooling, partial deep-crustal unroofing, or angular unconformities or normal faulting in the northeastern Basin and Range Province during the crucial pre-40-Ma time frame (e.g., Smith and Ketner 1978; Miller et al. 1987; Wells et al. 1990, 2000; Hodges and Walker 1992; Ketner and Alpha 1992; McGrew and Snee 1994; Brooks et al. 1995; Potter et al. 1995; Dubiel et al. 1996; Camilleri and Chamberlin 1997; Wells 1997; McGrew et al. 2000*a*). However, despite these efforts to document older crustal thinning, few, if any, surface-breaking normal faults in northeastern Nevada have been firmly documented to significantly predate the Late Eocene. If crustal thinning did occur before this time frame, it may have been mediated by processes other than surface-breaking normal faults, such as deep-crustal flow (e.g., McGrew et al. 2000*a*).

The crustal gravitational-collapse hypothesis is further weakened by evidence suggesting that the crust of northeastern Nevada was not especially overthickened by Middle Eocene time. As pointed out by Jones et al. (1998), gravitational collapse requires regional elevations of at least 2–3 km, assuming a crustal thickness of 50–70 km and an average crustal density of 2.8 g/cm^3. Several recent paleobotanical investigations that include the Copper Basin flora (e.g., Povey et al. 1994; Wolfe et al. 1998) conclude that the elevation of the basin during the Eocene was similar to what it is today, ~2 km. Although these studies of paleoelevation are subject to large uncertainties and are hampered by the sparsity of the fossil record, they do not support the dramatic reduction in surface elevation that gravitational collapse predicts.

Evidence for a widespread, low-relief landscape in northeastern Nevada further challenges the proposition of excessively thickened crust and high surface elevations before Late Eocene extension. Of particular concern is the origin of the lacustrine deposits, the Elko and White Sage Formations, that

are widely distributed across Elko County and that appear to predate the onset of extension (Brooks et al. 1995; Dubiel et al. 1996). These lake beds consist mostly of fine-grained facies that suggest a low-relief landscape. They occur primarily in two depocenters: one in the vicinity of Elko in western Elko County (the Elko Basin; Solomon et al. 1979; Solomon and Moore 1982*a*, 1982*b*) and the other near Gold Hill along the Nevada-Utah state line (the White Sage Basin; Dubiel et al. 1996). However, sporadic outcrops of ostracodal lacustrine limestone also occur between the two major depocenters raising the possibility that they may once have been connected in a regionally extensive lake system (Brooks et al. 1995; Potter et al. 1995; Dubiel et al 1996). Throughout Elko County, these strata are deposited on Upper Paleozoic or Mesozoic strata, indicating that regional denudation of the landscape and partitioning into relatively small, discrete basins had not yet begun by Early Eocene time, and the strata record no definitive evidence of nearby tectonism at this time (Dubiel et al. 1996).

Taken together, these results suggest that the seminal event triggering the onset of regional extension in the northern Basin and Range Province was not crustal gravitational collapse but rather lithospheric thermal weakening recorded by the southward-sweeping passage of the volcanic front. In this view, the mantle lithosphere was thinned and weakened as hot, upwelling asthenosphere flowed in to fill the southward-opening wedge created either by the steepening and foundering of the subducted plate (Lipman 1980) or by delamination of the Farallon slab (Humphreys 1995) at the end of Laramide time. Earlier thickening of the crust during Mesozoic orogenesis probably contributed to extension and may even have been a necessary precondition, but crustal overthickening alone was probably insufficient to trigger extensional collapse without thinning and weakening of the mantle lithosphere to provide additional gravitational potential energy (Liu and Shen 1998). Conversely, models that invoke thinning or disappearance of the dense mantle lid are compatible with buoyant uplift of the crust simultaneously with regional extension and volcanism (Jones et al. 1998). In addition to providing an active driving force for extension, asthenospheric upwelling would also amplify any tendencies toward intra-arc or retro-arc extension due to decelerating convergence rates at the plate boundary starting at about 50 Ma (Engebretson et al. 1985). Even if Late Cretaceous and Early Tertiary crustal thickness was modulated by gravitationally driven thinning, mantle processes would be required to create the modern Basin and Range province (Liu and Shen 1998; Sonder and Jones 1999).

Conclusions

Starting at ~42 Ma, a pulse of silicic volcanism occurred throughout northeastern Nevada, represented by eruption of the tuffs within the Dead Horse Formation in the Copper Mountains area. This unit rests on upper Paleozoic strata and was early syntectonic with respect to the Copper Basin fault system, a significant normal fault with 8–12 km displacement based on restoration of a displaced slice of the Cretaceous Coffeepot Stock and its country rock. The Copper Basin fault system exhumed rocks from depths of ~11 ± 3 km. This system was subsequently modified by Miocene volcanism and associated small-scale extension.

The style and age of Paleogene tectonism in the Copper Mountains reinforce a regional pattern of southward-sweeping volcanism and extension from British Columbia to southern Nevada from Early Eocene to Late Oligocene time. Paleoelevation data and the existence of widespread Early Eocene lacustrine strata deposited on upper Paleozoic or Mesozoic rocks suggest that the crust of northeastern Nevada was only moderately thickened during the onset of Late Eocene extension. Consequently, gravitational instability due to crustal thickening was only a contributing factor and not the primary force driving the transition from regional contraction to extension. Rather, the key trigger mechanisms were probably changes in plate boundary conditions coupled with lithospheric weakening associated with regional magmatism.

ACKNOWLEDGMENTS

Funding for this research was provided by American Chemical Society Petroleum Research Fund Grant 33343-GB2; University of Dayton Research Council awards to A. J. McGrew; a National Science Foundation Council on Undergraduate Research fellowship awarded to Lindsey Griffith and A. J. McGrew; a University of Dayton Honors and Scholars Program award to J. M. Rahl; and a research grant from the North-Central Section of the Geological Society of America to J. M. Rahl. Leo Hickey provided valuable discussions on the interpretation of the paleoelevation data. Chris Henry and Karl Mueller are thanked for critical reviews that greatly improved the manuscript. Fritz Hubacher provided invaluable laboratory support for the $^{40}Ar/^{39}Ar$ geochronology.

REFERENCES CITED

Armstrong, R. L. 1968. Sevier orogenic belt in Nevada and Utah. Geol. Soc. Am. Bull. 79:429–458.

———. 1970. Geochronology of Tertiary igneous rocks, eastern Basin and Range province, western Utah, eastern Nevada and vicinity, U.S.A. Geochim. Cosmochim. Acta 34:203–232.

Armstrong, R. L., and Ward, P. 1991. Evolving geographic patterns of Cenozoic magmatism in the North-American Cordillera: the temporal and spatial association of magmatism and metamorphic core complexes. J. Geophys. Res. 96:13,201–13,224.

Axelrod, D. I. 1966. The eocene copper basin flora of northeastern Nevada. Univ. Calif. Publ. Geol. Sci. 59, 124 p.

Axen, G. J.; Taylor, W. J.; and Bartley, J. M. 1993. Space-time patterns and tectonic controls of Tertiary extension and magmatism in the Great Basin of the western United States. Geol. Soc. Am. Bull. 105:56–76.

Best, M. G., and Christiansen, E. H. 1991. Limited extension during peak Tertiary volcanism, Great-Basin of Nevada and Utah. J. Geophys. Res. 96: 13,509–13,528.

Brooks, W. E.; Thorman, C. H.; and Snee, L. W. 1995. $^{40}Ar/^{39}Ar$ ages and tectonic setting of the middle Eocene northeast Nevada volcanic field. J. Geophys. Res. 100:10,403–10,416.

Bushnell, K. O. 1967. Geology of the Rowland Quadrangle, Elko County, Nevada. Nev. Bur. Mines Geol. Bull. 67, 38 p.

Camilleri, P. A., and Chamberlin, K. R. 1997. Mesozoic tectonics and metamorphism in the Pequop Mountains and Wood Hills region, northeast Nevada: implications for the architecture and evolution of the Sevier orogen. Geol. Soc. Am. Bull. 109:74–94.

Carmichael, D. M. 1978. Metamorphic bathozones and bathograds: a measure of the depth of post-metamorphic uplift and erosion on the regional scale. Am. J. Sci. 278:769–797.

Coash, J. R. 1967. Geology of the Mount Velma Quadrangle, Elko County, Nevada. Nev. Bur. Mines Geol. Bull. 68, 20 p.

Coats, R. R. 1964. Geology of the Jarbidge Quadrangle, Nevada-Idaho. U.S. Geol. Surv. Bull. 1141–M, 24 p.

———. 1987. Geology of Elko County, Nevada. Nev. Bur. Mines Geol. Bull. 101, 112 p.

Coats, R. R., and Riva, J. F. 1983. Overlapping overthrust belts of late Paleozoic and Mesozoic ages, northern Elko County, Nevada. *In* Miller, D. M.; Todd, V. R.; and Howard, K. A., eds. Tectonic and stratigraphic studies in the eastern Great Basin. Geol. Soc. Am. Mem. 157:305–327.

Coney, P. J., and Harms, T. 1984. Cordilleran metamorphic core complexes: Cenozoic extensional relics of Mesozoic compression. Geology 12:550–554.

Coney, P. J., and Reynolds, S. J. 1977. Cordilleran Benioff zones. Nature 270:403–406.

Cross, T. A., and Pilger, R. H., Jr. 1978. Constraints on absolute motion and plate interaction inferred from Cenozoic igneous activity in the western United States. Am. J. Sci. 278:865–902.

Dubiel, R. F.; Potter, C. J.; Good, S. C.; and Snee, L. W. 1996. Reconstructing an Eocene extensional basin: the White Sage Formation, eastern Great Basin. *In* Beratan, K. K., ed. Reconstructing the history of Basin and Range extension using sedimentology and stratigraphy. Geol. Soc. Am. Spec. Pap. 303:1–14.

Engebretson, D. C.; Cox, A.; and Gordon, R. G. 1985. Relative motions between oceanic and continental plates in the Pacific Basin. Geol. Soc. Am. Spec. Pap. 206, 59 p.

Foster, D. A., and Fanning, C. M. 1997. Geochronology of the northern Idaho batholith and the bitterroot metamorphic core complex: magmatism preceding and contemporaneous with extension. Geol. Soc. Am. Bull. 109:379–394.

Gans, P. B.; Mahood, G. A.; and Schermer, E. 1989. Synextensional magmatism in the Basin and Range province: a case study from the eastern Great Basin. Geol. Soc. Am. Spec. Pap. 233, 53 p.

Gans, P. B.; Seedorff, E.; Fahey, P. L.; Hasler, R. W.; Maher, D. J.; Jeanne, R. A.; and Shaver, S. A. 2001. Rapid Eocene extension in the Robinson district, White Pine County, Nevada: constraints from $^{40}Ar/^{39}Ar$ dating. Geology 29:475–478.

Hodges, K. V., and Walker, J. D. 1992. Extension in the Cretaceous Sevier orogen, North American Cordillera. Geol. Soc. Am. Bull. 104:560–569.

Holdaway, M. J. 1971. Stability of andalusite and the aluminum phase diagram. Am. J. Sci. 271:97–131.

Houseman, G. A.; McKenzie, D. P.; and Molnar, P. 1981. Convective instability of a thickened boundary layer and its relevance for the thermal evolution of continental convergent belts. J. Geophys. Res. 86:6115–6132.

Humphreys, E. D. 1995. Post-Laramide removal of the Farallon Slab, Western United States. Geology 23:987–990.

Janecke, S. U. 1994. Sedimentation and paleogeography of an Eocene to Oligocene rift zone, Idaho and Montana. Geol. Soc. Am. Bull. 106:1083–1095.

Janecke, S. U.; Hammond, B. F.; Snee, L. W.; and Geissman, J. W. 1997. Rapid extension in an Eocene volcanic arc: structure and paleogeography of an intra-arc half graben in central Idaho. Geol. Soc. Am. Bull. 109:253–267.

Janecke, S. U., and Snee, L. W. 1993. Timing and episodicity of Middle Eocene volcanism and onset of conglomerate deposition, Idaho. J. Geol. 101:603–621.

Jones, C. H.; Sonder, L. J.; and Unruh, J. R. 1998. Lithospheric gravitational potential energy and past orogenesis: implications for conditions of initial Basin and Range and Laramide deformation. Geology 26:639–642.

Ketner, K. B. 1998. The nature and timing of tectonism in the western facies terrane of Nevada and California—an outline of evidence and interpretations de-

rived from geologic maps of key areas. U.S. Geol. Surv. Prof. Pap. 1592, 19 p.

Ketner, K. B., and Alpha, A. G. 1992. Mesozoic and Tertiary rocks near Elko, Nevada; evidence for Jurassic to Eocene folding and low-angle faulting. U.S. Geol. Surv. Bull. 1988C, p. C1–C13.

Ketner, K. B.; Murchey, B. L.; Stamm, R. G.; and Wardlaw, B. R. 1993. Paleozoic and Mesozoic rocks of Mount Ichabod and Dorsey Canyon, Elko County, Nevada; evidence for post–Early Triassic emplacement of the Roberts Mountains and Golconda allochthons. U.S. Geol. Surv. Bull. 1988D, p. D1–D12.

Ketner, K. B.; Repetski, J. E.; Stamm, R. G.; and Wardlaw, B. R. 1995. Geologic map of the Rowland-Bearpaw Mountain area, Elko County, Nevada. U.S. Geol. Surv. Misc. Field Investig. I-2536, scale 1 : 24,000.

Lapointe, D. D.; Tingley, J. V.; and Jones, R. B. 1991. Mineral resources of Elko County Nevada. Nev. Bur. Mines Geol. Bull. 106, 236 p.

Lipman, P. W. 1980. Cenozoic volcanism in the western United States: implications for continental tectonics. *In* Burchfiel, B. C.; Oliver, J. E.; and Silver, L. T., eds. Studies in geophysics, continental tectonics. Washington, D.C., National Academy of Sciences, p. 161–174.

Lipman, P. W.; Protska, H. J.; and Christiansen, R. L. 1972. Cenozoic volcanism and plate tectonic evolution of the western United States. 1. Early and middle Cenozoic. Philos. Trans. R. Soc. Lond. A Math. Phys. Sci. 271:217–248.

Little, T. A. 1987. Stratigraphy and structure of metamorphosed upper Paleozoic rocks near Mountain City, Nevada. Geol. Soc. Am. Bull. 98:1–17.

Liu, M., and Shen, Y. 1998. Crustal collapse, mantle upwelling, and Cenozoic extension in the North American Cordillera. Tectonics 17:311–321.

Malde, H. E., and Powers, H. A. 1962. Upper Cenozoic stratigraphy of western Snake River Plain, Idaho. Geol. Soc. Am. Bull. 73:1197–1219.

McGrew, A. J., and Snee, L. W. 1994. $^{40}Ar/^{39}Ar$ thermochronometric constraints on the tectonothermal evolution of the northern East Humboldt Range metamorphic core complex, Nevada. Special issue on late orogenic extension. Tectonophysics 238:425–450.

McGrew, A. J.; Peters, M. T.; and Wright, J. E. 2000*a*. Thermobarometric constraints on the tectonothermal evolution of the East Humboldt Range metamorphic core complex, Nevada. Geol. Soc. Am. Bull. 112:45–60.

McGrew, A. J.; Vanderbeek, G. A.; and Ali, O. E. 2000*b*. New insights into the deformational history of the Sevier hinterland from the Copper Mountains, northeastern Nevada. Geol. Soc. Am. Abstr. Program 32:A–170.

Miller, D. M.; Hillhouse, W. C.; Zartman, R. E.; and Lanphere, M. A. 1987. Geochronology of intrusive and metamorphic rocks in the Pilot Range, Utah and Nevada, and comparison with regional patterns. Geol. Soc. Am. Bull. 99:866–879.

Mueller, K. J.; Cerveny, P. K.; Perkins, M. E.; and Snee, L. W. 1999. Chronology of polyphase extension in the Windermere Hills, northeast Nevada. Geol. Soc. Am. Bull. 111:11–27.

Naney, M. T. 1983. Phase equilibria of rock-forming ferromagnesian silicates in granitic systems. Am. J. Sci. 283:993–1033.

Parrish, R. R.; Carr, S. D.; and Parkinson, D. L. 1988. Eocene extensional tectonics and geochronology of the southern Omineca Belt, British Columbia and Washington. Tectonics 7:181–212.

Platt, J. P., and England, P. C. 1994. Convective removal of lithosphere beneath mountain belts: thermal and mechanical consequences. Am. J. Sci. 294:307–336.

Potter, C. J.; Dubiel, R. F.; Snee, L. W.; and Good, S. C. 1995. Eocene extension of early Eocene lacustrine strata in a complexly deformed Sevier-Laramide hinterland, northwest Utah and northeast Nevada. Geology 23:181–184.

Povey, D. A. R.; England, P. C.; and Spicer, R. A. 1994. Palaeobotanical investigation of early Tertiary palaeoelevations in northeastern Nevada: initial results. Rev. Palaeobot. Palynol. 81:1–10.

Smith, J. F., Jr., and Ketner, K. B. 1978. Geologic map of the Carlin-Piñon Range area, Elko and Eureka counties, Nevada. U.S. Geol. Surv. Misc. Field Investig. I-1028, scale 1 : 24,000.

Solomon, B. J.; McKee, E. H.; and Anderson, D. W. 1979. Stratigraphy and depositional environments of Paleogene rocks near Elko, Nevada. *In* Armentrout, J. M.; Cole, M. R.; and TerBest, H., eds. Cenozoic Paleogeography of the western United States. Society of Economic Paleontologists and Mineralogists, Pacific Section, Pacific Coast Paleogeography Symposium 3:75–88.

Solomon, B. J., and Moore, S. W. 1982*a*. Geologic map and oil shale deposits of the Elko East quadrangle, Elko County, Nevada. U.S. Geol. Surv. Misc. Field Investig. MF-1421, scale 1 : 24,000.

———. 1982*b*. Geologic map and oil shale deposits of the Elko West quadrangle, Elko County, Nevada. U.S. Geol. Surv. Misc. Field Investig. MF-1410, scale 1 : 24,000.

Sonder, L. J., and Jones, C. H. 1999. Western United States extension: how the west was widened. Annu. Rev. Earth Planet. Sci. 27:417–462.

Wells, M. L. 1997. Alternating contraction and extension in the hinterlands of orogenic belts: an example from the Raft River Mountains, Utah. Geol. Soc. Am. Bull. 109:107–126.

Wells, M. L.; Dallmeyer, R. D.; and Allmendinger, R. W. 1990. Late Cretaceous extension in the hinterland of the Sevier thrust belt, northwestern Utah and southern Idaho. Geology 18:929–933.

Wells, M. L.; Snee, L. W.; and Blythe, A. E. 2000. Dating of major normal fault systems using thermochronology; an example from the Raft River detachment, Basin and Range, western United States. J. Geophys. Res. 105:16,303–16,327.

Wolfe, J. A.; Forest, C. E.; and Molnar, P. 1998. Paleobotanical evidence of Eocene and Oligocene paleoaltitudes in midlatitude western North America. Geol. Soc. Am. Bull. 110:664–678.